



# Development and validation of an MRI-based nomogram for the preoperative prediction of tumor mutational burden in lower-grade gliomas

En-Tao Liu<sup>1#^</sup>, Shuqin Zhou<sup>2#</sup>, Yingwen Li<sup>2#</sup>, Siwei Zhang<sup>2#</sup>, Zelan Ma<sup>2#</sup>, Junbiao Guo<sup>2#</sup>, Lei Guo<sup>2#</sup>, Yue Zhang<sup>2#</sup>, Quanlai Guo<sup>2#</sup>, Li Xu<sup>2^</sup>

<sup>1</sup>WeiLun PET Center, Department of Nuclear Medicine, Guangdong Provincial People's Hospital, Guangdong Academy of Medical Sciences, Guangzhou, China; <sup>2</sup>The Second Affiliated Hospital of Guangzhou University of Chinese Medicine and Guangdong Provincial Hospital of Chinese Medicine, Guangzhou, China

*Contributions:* (I) Conception and design: L Xu; (II) Administrative support: ET Liu; (III) Provision of study materials or patients: S Zhou, Y Li, S Zhang; (IV) Collection and assembly of data: Z Ma, Q Guo, J Guo; (V) Data analysis and interpretation: L Guo, Y Zhang; (VI) Manuscript writing: All authors; (VII) Final approval of manuscript: All authors.

#These authors contributed equally to this work.

*Correspondence to:* Li Xu, MD. The Second Affiliated Hospital of Guangzhou University of Chinese Medicine and Guangdong Provincial Hospital of Chinese Medicine, 111 Da De Lu, Guangzhou 510120, China. Email: 985592610@qq.com.

**Background:** High tumor mutational burden (TMB) is an emerging biomarker of sensitivity to immune checkpoint inhibitors. In this study, we aimed to determine the value of magnetic resonance (MR)-based preoperative nomogram in predicting TMB status in lower-grade glioma (LGG) patients.

**Methods:** Overall survival (OS) data were derived from The Cancer Genome Atlas (TCGA) and then analyzed by using the Kaplan-Meier method and time-dependent receiver operating characteristic (tdROC) analysis. The magnetic resonance imaging (MRI) data of 168 subjects obtained from The Cancer Imaging Archive (TCIA) were retrospectively analyzed. The correlation was explored by univariate and multivariate regression analyses. Finally, we performed tenfold cross validation. TMB values were retrieved from the supplementary information of a previously published article.

**Results:** The high TMB subtype was associated with the shortest median OS (high *vs.* low: 50.9 *vs.* 95.6 months,  $P < 0.05$ ). The tdROC for the high-TMB tumors was 74% (95% CI: 61–86%) for survival at 12 months, and 71% (95% CI: 60–82%) for survival at 24 months. Multivariate logistic regression analysis confirmed that three risk factors [extranodular growth: odds ratio (OR): 8.367, 95% CI: 3.153–22.199,  $P < 0.01$ ; length-width ratio  $\geq$  median: OR: 1.947, 95% CI: 1.025–3.697,  $P < 0.05$ ; frontal lobe: OR: 0.455, 95% CI: 0.229–0.903,  $P < 0.05$ ] were significant independent predictors of high-TMB tumors. The nomogram showed good calibration and discrimination. This model had an area under the curve (AUC) of 0.736 (95% CI: 0.655–0.817). Decision curve analysis (DCA) demonstrated that the nomogram was clinically useful. The average accuracy of the tenfold cross validation was 71.6% for high-TMB tumors.

**Conclusions:** Our results indicated that a distinct OS disadvantage was associated with the high TMB group. In addition, extranodular growth, nonfrontal lobe tumors and length-width ratio  $\geq$  median can be conveniently used to facilitate the prediction of high-TMB tumors.

**Keywords:** Nomogram; glioma; radiogenomics; tumor mutational burden

<sup>^</sup> ORCID: En-Tao Liu, 0000-0002-0388-5540; Li Xu, 0000-0001-7024-340.

Submitted Mar 17, 2021. Accepted for publication Aug 30, 2021.

doi: 10.21037/qims-21-300

View this article at: <https://dx.doi.org/10.21037/qims-21-300>

## Introduction

Lower-grade gliomas (LGGs) are a heterogeneous group of primary glial brain tumors with highly variable overall survival (OS) (1-3). The management of LGG (WHO grade II and III) is still controversial because LGG is molecularly distinct. Patients with similar clinical features may have diverse outcomes (4,5). However, the clinical significance of some newer biomarkers discovered by genomic studies has not been fully investigated (6,7). Intratumor genetic heterogeneity plays a pivotal role in driving disease progression and therapeutic resistance in LGG (8,9). Intratumor heterogeneity has been linked to metastatic potential and is likely to be an important prognostic feature of human cancer.

While treating cancer with immunotherapy can be highly effective, only some patients respond to these treatments (10,11). Given the promise that these agents have demonstrated in the treatment of refractory disease and the durable responses that occur in some patients, there is great interest in identifying the patients who are most likely to benefit from these therapies. One emerging biomarker for the response to anti-programmed cell death protein 1 (PD-1) therapy is tumor mutational burden (TMB). TMB, the total number of somatic coding mutations in a tumor, is emerging as a promising biomarker for immunotherapy response in cancer patients (12,13). High TMB is an emerging biomarker of sensitivity to immune checkpoint inhibitors and has been shown to be more significantly associated with the response to PD-1 inhibitors and programmed death-ligand 1 (PD-L1) blockade immunotherapy than PD-1 or PD-L1 expression, as measured by immunohistochemistry (IHC) (14,15).

From diagnostics to prognosis to response prediction, new applications for radiogenomics are rapidly being developed (16-18). Radiogenomics aims to correlate radiological features with gene mutations, gene expression patterns, and other genome-related features and is designed to capture the intrinsic tumor heterogeneity and facilitate a deeper understanding of tumor biology (18,19). However, no study has investigated the associations among TMB, magnetic resonance imaging (MRI) features and OS in LGG. In this study, we used TMB to measure heterogeneity and investigated its correlation with MRI features and

survival outcomes.

## Methods

### Patients

The study was conducted in accordance with the Declaration of Helsinki (as revised in 2013). All patient data was acquired from the published The Cancer Genome Atlas LGG (TCGA-LGG) project and within this publication it is stated "Specimens were obtained from patients, with appropriate consent from institutional review boards" (<http://cancergenome.nih.gov/>). The publicly available clinical data used in this study were released by TCGA. For each patient, the determination of age, laterality, gender, race category, method of sample procurement, first presenting symptom, seizure, neoplasm histologic grade and histological type were based on file "nationwidechildrens.org\_clinical\_patient\_lgg" downloaded from <https://tcga-data.nci.nih.gov/tcga/dataAccessMatrix.htm>. For the subset of the LGG patients from TCGA, the MR exams were made available by The Cancer Imaging Archive (TCIA) (<https://wiki.cancerimagingarchive.net/>). All adult patients with LGG were retrospectively reviewed. Patients were only included if they met all of the following inclusion criteria: (I) LGG was confirmed by histopathology; (II) patients underwent MRI (TCIA); and (III) TMB values were available (TCGA). The TMB value of each patient was derived from previously published articles (20). A total of 168 patients (60 with high-TMB gliomas and 108 with low-TMB gliomas) fit the inclusion criteria.

### Radiologist review of the MR image features

By referring to previous studies (21-23) the following 20 qualitative imaging descriptors were evaluated: (I) volume (<60 cm<sup>3</sup> versus ≥60 cm<sup>3</sup>); (II) multifocality (no versus yes); (III) intratumoral hemorrhage (no versus yes); (IV) enhancing margin (well defined margin versus poorly-defined margin); (V) necrosis (no versus yes); (VI) proportion contrast-enhanced (CE) tumor (<5% versus ≥5%); (VII) subventricular zone (SVZ) involvement (no versus yes): the tumors located in close contact with the SVZ are classified as SVZ +, while the tumors located

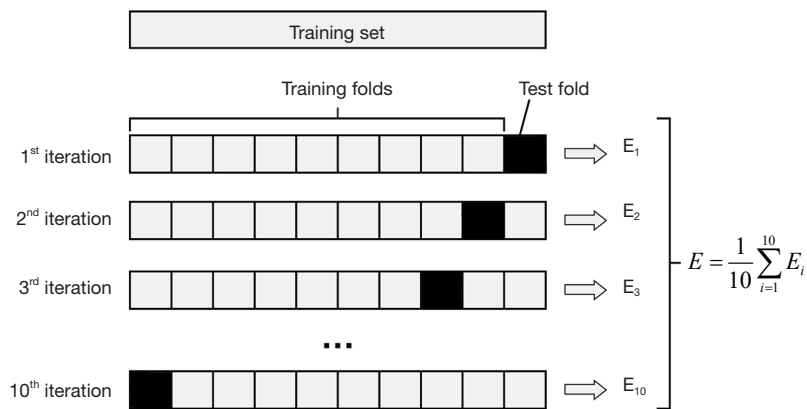


**Figure 1** Illustration of ten-fold cross validation.

distantly from the SVZ are classified as SVZ –; (VIII) multilobar lesions (no versus yes); (IX) extranodular growth (no versus yes); (X) T1 + C/T2 mismatch (no versus yes); (XI) depth (< median or ≥ median); (XII) width (< median or ≥ median); (XIII) length (< median or ≥ median); (XIV) volume (< median or ≥ median); (XV) length (< median or ≥ median); (XVI) the shortest distance between the edge of the lateral and the tumor centroid (CS) (≤30 mm or >30 mm); (XVII) length-width ratio (< median or ≥ median); (XVIII) length-depth ratio (< median or ≥ median); (XIX) width-depth ratio (< median or ≥ median); (XX) location (frontal lobe versus other).

The readers independently made their classifications based on the MR images, and in cases of disagreement, a consensus was reached after discussion. Both evaluators were blinded to patient's data. The interobserver and intraobserver reproducibility of LGG MR features has been reported in our previous work (24).

### Statistical analysis

The patients were divided into low and high TMB groups according to previously published articles. The OS data of each patient were derived from the TCGA. The relationship between intratumor genetic heterogeneity and OS was assessed using Kaplan-Meier analysis and time-dependent receiver operating characteristic (tdROC) analysis (R package). The correlations between TMB and MRI features were explored. A univariate analysis of variables was carried out using the chi-square test (or Fisher's exact test as appropriate). Binary logistic regression analyses (version 23.0; SPSS Company, Chicago, IL, USA) were performed

to identify independent factors of intratumoral genetic heterogeneity (high-TMB group or low-TMB group). The estimated odds ratio (OR) was reported. Two-sided  $P < 0.05$  indicated a significant difference. The discrimination of the models was assessed. It was measured using the receiver operating characteristic curve and summarized by the area under the curve (AUC). An AUC of 1.0 indicates perfect concordance, whereas an AUC of 0.5 indicates no relationship. Finally, we performed tenfold cross validation (Figure 1).

### Results

Of the 271 patients from the TCGA, 94 had high-TMB gliomas and 177 had low-TMB gliomas. High TMB-subtype was associated with shortest median OS (high *vs.* low: 50.9 *vs.* 95.6 months,  $P < 0.05$ ). OS were assessed using Kaplan-Meier analysis and tdROC analysis. Kaplan-Meier analysis (Figure 2A) indicated that there was a significant difference in OS between the high TMB tumors and low TMB tumors. The tdROC (Figure 2B) for the high TMB tumors was 0.74 (95% CI: 0.61–0.86) for survival at 12 months, and 0.71 (95% CI: 0.60–0.82) for survival at 24 months.

Of the 168 patients from the TCIA, 60 had high-TMB gliomas and 108 had low-TMB gliomas. The relations of selected patient clinical characteristics and MR characteristics to TMB groups are shown in Tables 1,2. Correlation matrix (Figure 3) yielded distinct groups of TMB status and qualitative MRI features of LGG. In univariate analysis, degree of enhancement, proportion CE tumor, extranodular growth, T1 + C/T2 mismatch, location,

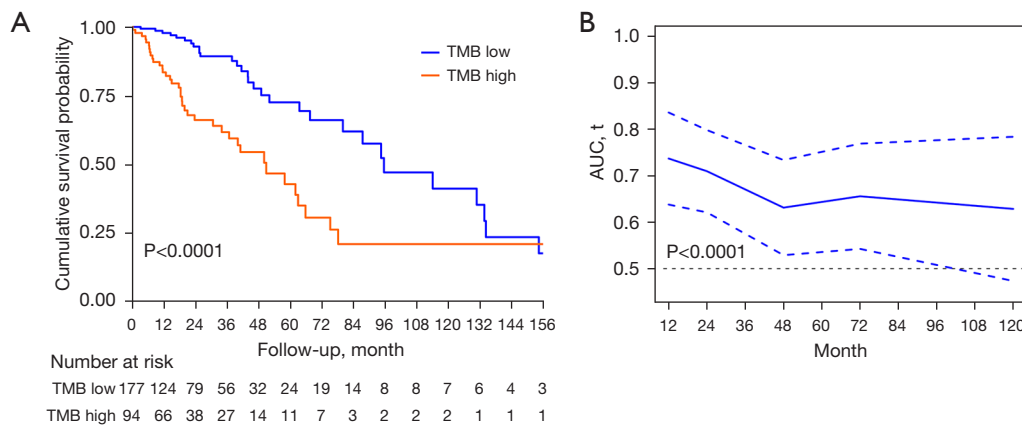


**Figure 2** OS were assessed using Kaplan-Meier analysis (A). The tdROC (B, dotted dash lines: 95% CI) for the high TMB tumors was 0.74 (95% CI: 0.61–0.86) for survival at 12 months, and 0.71 (95% CI: 0.60–0.82) for survival at 24 months. TMB, tumor mutational burden; AUC, area under the curve; OS, overall survival; tdROC, time-dependent receiver operating characteristic.

**Table 1** Clinical characteristics of the LGG sample set according to TMB status

Characteristics	Total (n=168)	TMB group		$\chi^2/t$	P
		TMB low	TMB high		
Histological type, no. (%)				1.978	0.372
Oligodendroglioma	69 (41.82)	46 (42.59)	23 (40.35)		
Astrocytoma	56 (33.94)	33 (30.56)	23 (40.35)		
Oligoastrocytoma	40 (24.24)	29 (26.85)	11 (19.3)		
Neoplasm histologic grade, no. (%)				11.435	0.001
GII	82 (49.7)	64 (59.26)	18 (31.58)		
GIII	83 (50.3)	44 (40.74)	39 (68.42)		
Age at diagnosis, years				-8.258	<0.001
Mean	43.86±13.53	38.54±11.65	53.95±10.9		
Range	20–75	20–74	22–75		
Gender, no. (%)				3.942	0.047
Female	78 (47.27)	45 (41.67)	33 (57.89)		
Male	87 (52.73)	63 (58.33)	24 (42.11)		
Race, no. (%)				-	0.302
American Indian or Alaska native	1 (0.61)	1 (0.93)	0 (0)		
Black or African American	11 (6.71)	5 (4.67)	6 (10.53)		
White	152 (92.68)	101 (94.39)	51 (89.47)		
Family history of cancer, no. (%)				0.88	0.348
No	67 (53.60)	48 (56.47)	19 (47.50)		
Yes	58 (46.40)	37 (43.53)	21 (52.50)		

**Table 1** (continued)

Table 1 (continued)

Characteristics	Total (n=168)	TMB group		$\chi^2/t$	P
		TMB low	TMB high		
Method of sample procurement, no. (%)				–	0.005
Open biopsy	6 (3.57)	4 (3.70)	2 (3.33)		
Subtotal resection	55 (32.74)	26 (24.07)	29 (48.33)		
Gross total resection	107 (63.69)	78 (72.22)	29 (48.33)		
First presenting symptom, no. (%)				7.64	0.106
Headaches	40 (25.00)	30 (28.57)	10 (18.18)		
Mental status change	15 (9.38)	6 (5.71)	9 (16.36)		
Motor or movement change	11 (6.88)	9 (8.57)	2 (3.64)		
Seizure	85 (53.13)	55 (52.38)	30 (54.55)		
Sensory or visual change	9 (5.63)	5 (4.76)	4 (7.27)		
Laterality, no. (%)				–	0.943
Left	79 (48.47)	52 (49.06)	27 (47.37)		
Midline	3 (1.84)	2 (1.89)	1 (1.75)		
Right	81 (49.69)	52 (49.06)	29 (50.88)		
IDH/1p19q subtype, no. (%)				22.295	<0.001
IDHmut-non-codel	85 (51.20)	63 (59.43)	22 (36.67)		
IDHmut-codel	43 (25.90)	31 (29.25)	12 (20.00)		
IDHwt	38 (22.89)	12 (11.32)	26 (43.33)		

LGG, lower-grade glioma; TMB, tumor mutational burden; IDHmut-non-codel, LGG with IDH mutation and no 1p/19q codeletion; IDHmut-codel, LGG with IDH mutation and 1p/19q codeletion; IDHwt, LGG with wild-type IDH.

Table 2 Summary of MR features per TMB-based subtypes

MR features	Total (n=168)	TMB group		$\chi^2$	P
		TMB low	TMB high		
Necrosis				0.149	0.700
Negative	31 (18.45)	19 (17.59)	12 (20.00)		
Positive	137 (81.55)	89 (82.41)	48 (80.00)		
Multifocality				10.388	0.001
Negative	161 (95.83)	108 (100.00)	53 (88.33)		
Positive	7 (4.17)	0 (0)	7 (11.67)		
Hemorrhage				0.101	0.750
Negative	142 (84.52)	92 (85.19)	50 (83.33)		
Positive	26 (15.48)	16 (14.81)	10 (16.67)		

Table 2 (continued)

Table 2 (continued)

MR features	Total (n=168)	TMB group		$\chi^2$	P
		TMB low	TMB high		
Degree of enhancement				8.925	0.003
Negative	68 (43.04)	52 (52.00)	16 (27.59)		
Positive	90 (56.96)	48 (48.00)	42 (72.41)		
Proportion CE tumor				12.984	<0.001
Negative	102 (64.56)	75 (75.00)	27 (46.55)		
Positive	56 (35.44)	25 (25.00)	31 (53.45)		
Enhancing margin				0.024	0.876
Well-defined	42 (26.58)	27 (27.00)	15 (25.86)		
Poorly-defined	116 (73.42)	73 (73.00)	43 (74.14)		
Extranodular growth				19.49	<0.001
Negative	129 (81.65)	92 (92.00)	37 (63.79)		
Positive	29 (18.35)	8 (8.00)	21 (36.21)		
T1 + C/T2 mismatch				6.763	0.009
Negative	135 (85.44)	91 (91.00)	44 (75.86)		
Positive	23 (14.56)	9 (9.00)	14 (24.14)		
CS				1.744	0.187
>30 mm	86 (51.81)	59 (55.66)	27 (45.00)		
≤30 mm	80 (48.19)	47 (44.34)	33 (55.00)		
Location				5.169	0.023
Other	104 (61.90)	60 (55.56)	44 (73.33)		
Frontal lobe	64 (38.10)	48 (44.44)	16 (26.67)		
SVZ				7.413	0.006
Negative	59 (35.12)	46 (42.59)	13 (21.67)		
Positive	109 (64.88)	62 (57.41)	47 (78.33)		
Volume				0.162	0.687
<60 cm <sup>3</sup>	50 (29.76)	31 (28.70)	19 (31.67)		
≥60 cm <sup>3</sup>	118 (70.24)	77 (71.30)	41 (68.33)		
Intratumoral vascular				0.001	0.973
Negative	4 (2.53)	2 (2.00)	2 (3.45)		
Positive	154 (97.47)	98 (98.00)	56 (96.55)		
Length				3.303	0.069
< median	83 (49.4)	59 (54.63)	24 (40.00)		
≥ median	85 (50.6)	49 (45.37)	36 (60.00)		

Table 2 (continued)

Table 2 (continued)

MR features	Total (n=168)	TMB group		$\chi^2$	P
		TMB low	TMB high		
Width				0.043	0.836
< median	83 (49.40)	54 (50.00)	29 (48.33)		
≥ median	85 (50.60)	54 (50.00)	31 (51.67)		
Depth				0.013	0.908
< median	83 (49.40)	53 (49.07)	30 (50.00)		
≥ median	85 (50.60)	55 (50.93)	30 (50.00)		
Length-width ratio				4.192	0.041
< median	85 (50.60)	61 (56.48)	24 (40.00)		
≥ median	83 (49.40)	47 (43.52)	36 (60.00)		
Length-depth ratio				0.305	0.581
< median	86 (51.19)	57 (52.78)	29 (48.33)		
≥ median	82 (48.81)	51 (47.22)	31 (51.67)		
Length-depth ratio				0.014	0.907
< median	84 (50.60)	54 (50.94)	30 (50.00)		
≥ median	82 (49.40)	52 (49.06)	30 (50.00)		
Volume				0.28	0.597
< median	83 (49.40)	55 (50.93)	28 (46.67)		
≥ median	85 (50.60)	53 (49.07)	32 (53.33)		

MR, magnetic resonance; TMB, tumor mutational burden; CE, contrast-enhanced; CS, the shortest distance between the edge of the lateral and the tumor centroid; SVZ, subventricular zone.

SVZ and length-width ratio were significant independent predictors of high TMB tumors ( $P < 0.05$ ).

Multivariate logistic regression analysis confirmed that three risk factors (extranodular growth: OR: 8.367, 95% CI: 3.153–22.199,  $P < 0.01$ ; length-width ratio  $\geq$  median: OR: 1.947, 95% CI: 1.025–3.697,  $P < 0.05$ ; frontal lobe: OR: 0.455, 95% CI: 0.229–0.903,  $P < 0.05$ ) were significant independent predictors of high TMB tumors (Table 3). Extranodular growth, nonfrontal lobe tumors and length-width ratio  $\geq$  median were associated with a significantly higher incidence of high TMB tumors (Figure 4). After multivariate analysis, the nomogram was built. The nomogram (Figure 5) showed good calibration and discrimination. The AUC for the ROC curve was 0.736 (95% CI: 0.655–0.817) for high TMB tumors (Figure 6A). Decision curve analysis (DCA) demonstrated that the nomogram was clinically useful (Figure 6B). The average

accuracy of the tenfold cross validation was 71.6% for high TMB tumors.

Subgroup analysis (Table 4) of IDHmut-non-codel subtype ( $n=85$ ) found that SVZ and extranodular growth were significant independent predictors of high TMB tumors ( $P < 0.05$ ). Multivariate logistic regression analysis confirmed that extranodular growth (OR: 4.297, 95% CI: 1.031–17.916,  $P < 0.05$ ) was still the independent predictive factor for TMB tumors.

## Discussion

LGG form a biologically heterogeneous group of tumors. Intratumoral genetic heterogeneity, variation within a patient's individual tumor cells, is increasingly seen as a molecular mechanism underlying therapeutic failure and treatment resistance (25). Recently, checkpoint inhibitors

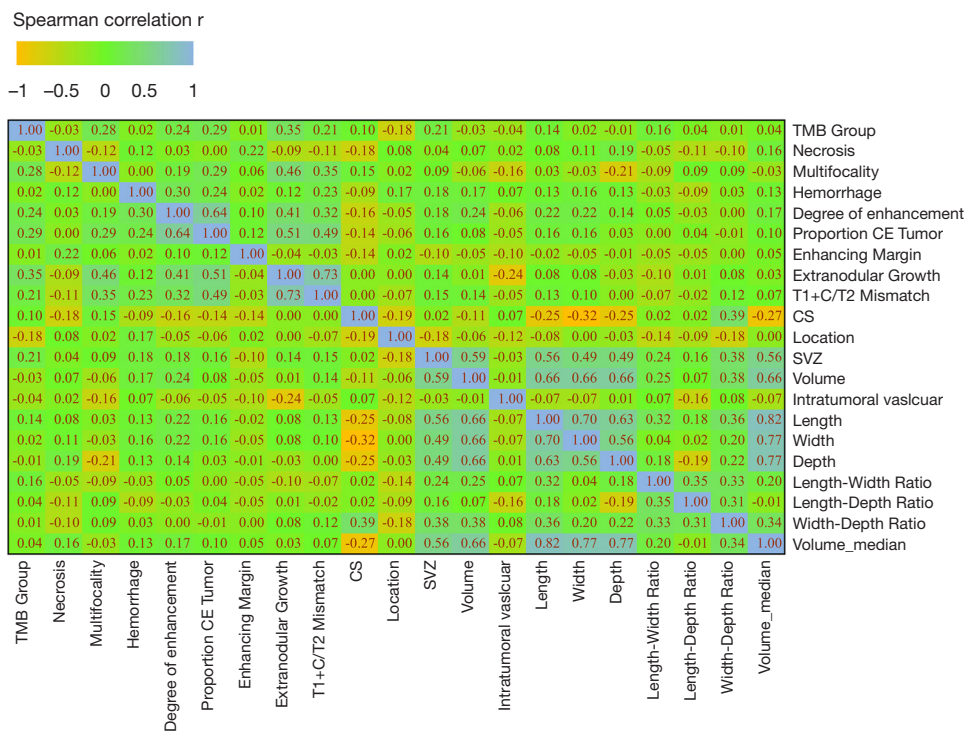


**Figure 3** Correlation matrix of qualitative MR features and TMB status. TMB, tumor mutational burden; CE, contrast-enhanced; CS, the shortest distance between the edge of the lateral and the tumor centroid; SVZ, subventricular zone; MR, magnetic resonance.

(PD-L1 or PD-1 inhibitors) have emerged as potential therapeutic options for adult and pediatric gliomas (26,27). TMB is well known to predict the response to immune checkpoint inhibitors (28,29). Highly mutated tumors are thought to harbor an increased neoantigen burden, making them immunogenic and responsive to immunotherapy (30).

Predicting TMB tumors in low-grade glioma patients is of great clinical importance, as it can potentially help better manage such patients and develop personalized treatment plans. The idea of using MRI is also appealing, as it is already part of the standard clinical diagnostic routine for this population, so the lack of an additional cost/procedure may make potential clinical translation easier. A meta-analysis (n=103,078) showed that for various cancer patients treated with surgery or chemotherapy, the prognostic role of TMB was dependent on cancer type. The meta-analysis (n=103,078) showed that regarding the response to immune checkpoint therapy, the high-TMB group had a significantly higher response rate than the low-TMB group.

There are a number of reports regarding MRI-based

**Table 3** Results from risk analyses (univariate and multivariate logistic regression, ORs, 95% CI in parentheses)

MR features	Univariate logistic regression	Multivariate logistic regression
Necrosis		
Negative	Reference	
Positive	0.854 (0.382–1.907)	
Multifocality		
Negative	Reference	
Positive	–	
Hemorrhage		
Negative	Reference	
Positive	1.15 (0.486–2.723)	
Degree of enhancement		
Negative	Reference	
Positive	2.844 (1.417–5.708)**	

**Table 3** (continued)

Table 3 (continued)

MR features	Univariate logistic regression	Multivariate logistic regression
Proportion CE tumor		
Negative	Reference	
Positive	3.444 (1.734–6.842)***	
Enhancing margin		
Well-defined	Reference	
Poorly-defined	1.06 (0.508–2.211)	
Extranodular growth		
Negative	Reference	
Positive	6.527 (2.656–16.042)***	8.367 (3.153–22.199)**
T1 + C/T2 mismatch		
Negative	Reference	
Positive	3.217 (1.293–8.004)*	
CS		
>30 mm	Reference	
≤30 mm	1.534 (0.812–2.9)	
Location		
Other	Reference	
Frontal lobe	0.455 (0.229–0.903)*	0.458 (0.212–0.991)*
SVZ		
Negative	Reference	
Positive	2.682 (1.302–5.527)**	
Volume		
<60 cm <sup>3</sup>	Reference	
≥60 cm <sup>3</sup>	0.869 (0.438–1.724)	
Intratumoral vascular		
Negative	Reference	
Positive	0.571 (0.078–4.169)	
Length		
< median	Reference	
≥ median	1.806 (0.952–3.427)	
Width		
< median	Reference	
≥ median	1.069 (0.569–2.01)	

Table 3 (continued)

Table 3 (continued)

MR features	Univariate logistic regression	Multivariate logistic regression
Depth		
< median	Reference	
≥ median	0.964 (0.513–1.812)	
Length-width ratio		
< median	Reference	
≥ median	1.947 (1.025–3.697)*	2.39 (1.128–5.066)*
Length-depth ratio		
< median	Reference	
≥ median	1.195 (0.635–2.247)	
Length-depth ratio		
< median	Reference	
≥ median	1.038 (0.551–1.956)	
Volume		
< median	Reference	
≥ median	1.186 (0.63–2.232)	

\*, P<0.05; \*\*, P<0.01; \*\*\*, P<0.001. ORs, odds ratios; MR, magnetic resonance; CE, contrast-enhanced; CS, the shortest distance between the edge of the lateral and the tumor centroid; SVZ, subventricular zone.

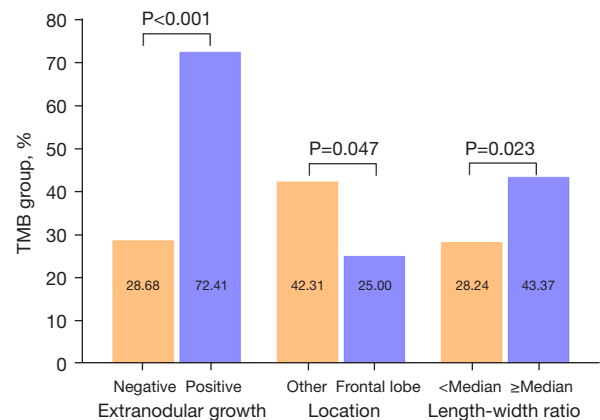
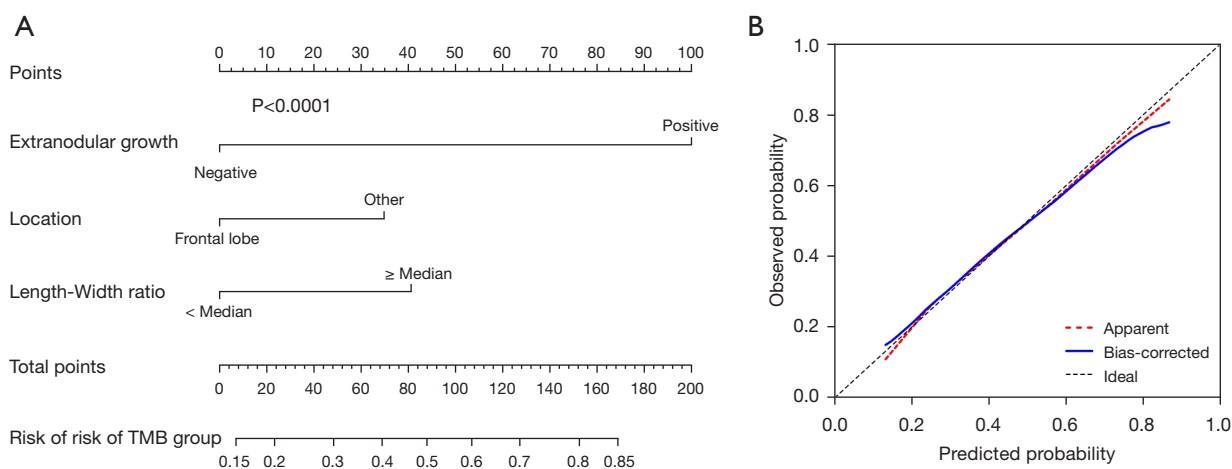
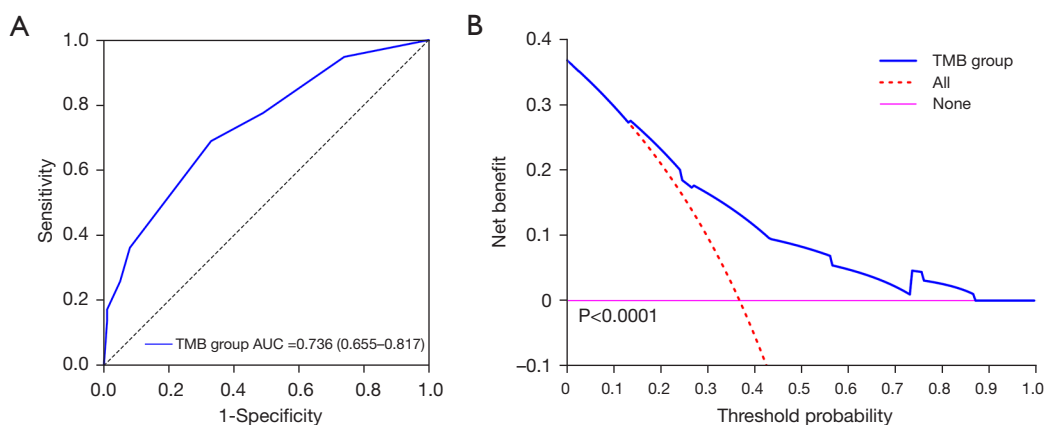


Figure 4 Extranodular growth, nonfrontal lobe tumors and length-width ratio ≥ median were associated with a significantly higher incidence of high TMB tumors. TMB, tumor mutational burden.



**Figure 5** The nomogram (A) showed good discrimination and was well calibrated. (B) The calibration curve showed that the nomogram achieved good agreement between prediction and actual observation. TMB, tumor mutational burden.



**Figure 6** The ROC and DCA demonstrated the usefulness of the proposed nomogram. TMB, tumor mutational burden; AUC, area under the curve; ROC, receiver operating characteristic; DCA, decision curve analysis.

prediction models for LGG. Wei and coworkers found that a radiomics signature accurately predicted MGMT promoter methylation in patients with astrocytomas and achieved survival stratification for TMZ chemotherapy (31). Broen and coworkers confirmed that among nonenhancing LGG, the T2-FLAIR mismatch sign represents a highly specific imaging marker for IDH-mutant astrocytoma (32). Wang and coworkers found that a radiomics signature was independent of clinicopathologic data and was a noninvasive pretreatment predictor for LGG patient survival (33). Tay and coworkers confirmed the possibility of a primary cerebral neoplasm representing a protoplasmic astrocytoma in a patient with a large frontal or temporal tumor that has a

very high signal on T2 with a large proportion of the tumor showing substantial T2 FLAIR suppression (34).

There are a number of reports regarding the relationship between prognosis and TMB. Alghamri and coworkers (35) found that TMB is negatively associated with clinical outcomes in metastatic patients with EGFR-mutant lung cancer treated with EGFR tyrosine kinase inhibitors. Samstein and coworkers (36) demonstrated that TMB is associated with improved survival in patients receiving immune checkpoint inhibitors across a wide variety of cancer types. Hwang and coworkers (37) found that the mutational burden of primary neuroblastoma may be useful in combination with conventional risk factors to optimize

**Table 4** Results from risk analyses (univariate and multivariate logistic regression, ORs, 95% CI in parentheses IDHmut-non-codel n=85)

MR features	Univariate logistic regression	Multivariate logistic regression
Necrosis		
Negative	Reference	
Positive	1.059 (0.303–3.706)	
Hemorrhage		
Negative	Reference	
Positive	0.702 (0.074–6.645)	
Degree of enhancement		
Negative	Reference	
Positive	1.806 (0.638–5.117)	
Proportion CE tumor		
Negative	Reference	
Positive	1.402 (0.495–3.968)	
Enhancing margin		
Well-defined	Reference	
Poorly-defined	0.941 (0.225–3.939)	
Extranodular growth		
Negative	Reference	
Positive	4.297 (1.031–17.916)*	4.297 (1.031–17.916)*
T1 + C/T2 mismatch		
Negative	Reference	
Positive	2.292 (0.468–11.224)	
CS		
>30 mm	Reference	
≤30 mm	0.994 (0.362–2.725)	
Location		
Other	Reference	
Frontal lobe	0.447 (0.146–1.367)	
SVZ		
Negative	Reference	
Positive	4.167 (1.115–15.568)*	

**Table 4** (continued)**Table 4** (continued)

MR features	Univariate logistic regression	Multivariate logistic regression
Volume		
<60 cm <sup>3</sup>	Reference	
≥60 cm <sup>3</sup>	3.404 (0.715–16.206)	
Intratumoral vascular		
Negative	Reference	
Positive	0.702 (0.060–8.164)	
Length		
< median	Reference	
≥ median	2.900 (0.952–8.83)	
Width		
< median	Reference	
≥ median	1.641 (0.564–4.771)	
Depth		
< median	Reference	
≥ median	2.275 (0.787–6.572)	
Length-width ratio		
< median	Reference	
≥ median	2.679 (0.960–7.47)	
Length-depth ratio		
< median	Reference	
≥ median	1.313 (0.491–3.510)	
Width-depth ratio		
< median	Reference	
≥ median	1.239 (0.468–3.28)	
Volume		
< median	Reference	
≥ median	2.55 (0.836–7.776)	

\*, P<0.05. ORs, odds ratios; IDHmut-non-codel, lower-grade glioma with IDH mutation and no 1p/19q codeletion; MR, magnetic resonance; CE, contrast-enhanced; CS, the shortest distance between the edge of the lateral and the tumor centroid; SVZ, subventricular zone.

risk stratification and guide treatment decisions, pending prospective validation. Wang and coworkers (20) found that TMB is associated with poor outcomes in diffuse glioma, and the high proliferative activity in the high-TMB group could account for the shorter survival of these patients. However, no study has investigated associations between TMB and MRI features in LGG.

Radiogenomics is a computational discipline that identifies correlations between cross-sectional imaging features and tissue-based molecular data (38,39). Tumor size, tumor location, composition, and MRI features tend to demonstrate significant associations with genomic and molecular factors, likely related to the cell of origin and growth characteristics (39). Tumor heterogeneity (8) has been explored at the histological and genetic levels, and increased levels of intratumor genetic heterogeneity have been reported to be associated with adverse clinical outcomes. In the current study, the correlations between TMB status and MRI features were explored. Multivariate logistic regression analysis confirmed that extranodular growth, nonfrontal lobe tumors and length-width ratio  $\geq$  median can be conveniently used to facilitate the prediction of high-TMB tumors. The nomogram showed good discrimination (AUC: 0.732) for predicting high-TMB gliomas. To our knowledge, this is the first study focusing on the relationships among TMB status, MR features and OS in patients with LGG.

A meta-analysis showed that codeletion of 1p and 19q is associated with better survival rates in glioma (40). Another meta-analysis revealed that patients with glioma harboring IDH mutations have improved OS and progression free survival (PFS), especially patients with WHO grade III and grade II–III (41). TCGA Research Network classified LGG into three categories: LGG with IDH mutation and no 1p/19q codeletion (IDHmut-non-codel), LGG with IDH mutation and 1p/19q codeletion (IDHmut-codel), and LGG with wild-type IDH (IDHwt). The IDHmut-noncodel subtype is linked to the best OS. Subgroup analysis of the IDHmut-noncodel subtype (n=85) confirmed that extranodular growth was still an independent predictive factor of TMB tumors.

This study has several limitations. Tissue samples for the TCGA were collected from many sites and analyzed to reach accrual targets, with usually approximately five hundred specimens per cancer type. For this reason, the MR image data sets are heterogeneous in terms of MR scanner modalities, manufacturers and MR acquisition protocols. However, similar to other articles published using TCGA

datasets (42), the lesions were relatively large. In addition, an average accuracy of 71.6% was obtained based on the tenfold cross-validation method for high-TMB tumors. The result of the value was good. Therefore, we believe that our results are not largely affected by this limitation.

In conclusion, our results indicated that distinct OS disadvantages were associated with the high TMB group. Additionally, extranodular growth, nonfrontal lobe tumors and length-width ratio  $\geq$  median can be conveniently used to facilitate the prediction of high-TMB tumors. The calibration curve and DCA demonstrated the usefulness of the proposed nomogram. The average accuracy of the tenfold cross validation was 71.6% for high-TMB tumors.

### Acknowledgments

*Funding:* This study was supported by National Natural Science Foundation of China (grant No. 81801688) and Traditional Chinese Medicine Bureau of Guangdong Province (grant No. 20181116).

### Footnote

*Conflicts of Interest:* All authors have completed the ICMJE uniform disclosure form (available at <https://dx.doi.org/10.21037/qims-21-300>). The authors have no conflicts of interest to declare.

*Ethical Statement:* The authors are accountable for all aspects of the work in ensuring that questions related to the accuracy or integrity of any part of the work are appropriately investigated and resolved. The study was conducted in accordance with the Declaration of Helsinki (as revised in 2013). All patient data was acquired from the published TCGA-LGG project and within this publication it is stated “Specimens were obtained from patients, with appropriate consent from institutional review boards” (<http://cancergenome.nih.gov/>).

*Open Access Statement:* This is an Open Access article distributed in accordance with the Creative Commons Attribution-NonCommercial-NoDerivs 4.0 International License (CC BY-NC-ND 4.0), which permits the non-commercial replication and distribution of the article with the strict proviso that no changes or edits are made and the original work is properly cited (including links to both the formal publication through the relevant DOI and the license). See: <https://creativecommons.org/licenses/by-nc-nd/4.0/>.

## References

- Darlix A, Gozé C, Rigau V, Bauchet L, Taillandier L, Duffau H. The etiopathogenesis of diffuse low-grade gliomas. *Crit Rev Oncol Hematol* 2017;109:51-62.
- Ferracci FX, Michaud K, Duffau H. The landscape of postsurgical recurrence patterns in diffuse low-grade gliomas. *Crit Rev Oncol Hematol* 2019;138:148-55.
- Delgado-López PD, Corrales-García EM, Martino J, Lastra-Aras E, Dueñas-Polo MT. Diffuse low-grade glioma: a review on the new molecular classification, natural history and current management strategies. *Clin Transl Oncol* 2017;19:931-44.
- Morshed RA, Young JS, Hervey-Jumper SL, Berger MS. The management of low-grade gliomas in adults. *J Neurosurg Sci* 2019;63:450-7.
- Smits A, Jakola AS. Clinical Presentation, Natural History, and Prognosis of Diffuse Low-Grade Gliomas. *Neurosurg Clin N Am* 2019;30:35-42.
- Jakola AS, Unsgård G, Kloster R, Solheim O. Diffuse low-grade gliomas. *J Neurosurg* 2013;119:1354-5.
- Garcia CR, Slone SA, Pittman T, St Clair WH, Lightner DD, Villano JL. Comprehensive evaluation of treatment and outcomes of low-grade diffuse gliomas. *PLoS One* 2018;13:e0203639.
- McGranahan N, Swanton C. Clonal Heterogeneity and Tumor Evolution: Past, Present, and the Future. *Cell* 2017;168:613-28.
- Prasetyanti PR, Medema JP. Intra-tumor heterogeneity from a cancer stem cell perspective. *Mol Cancer* 2017;16:41.
- Prieto PA, Yang JC, Sherry RM, Hughes MS, Kammula US, White DE, Levy CL, Rosenberg SA, Phan GQ. CTLA-4 blockade with ipilimumab: long-term follow-up of 177 patients with metastatic melanoma. *Clin Cancer Res* 2012;18:2039-47.
- Crow J, Samuel G, Godwin AK. Beyond tumor mutational burden: potential and limitations in using exosomes to predict response to immunotherapy. *Expert Rev Mol Diagn* 2019;19:1079-88.
- Fancelli L, Gandini S, Pelicci PG, Mazzarella L. Tumor mutational burden quantification from targeted gene panels: major advancements and challenges. *J Immunother Cancer* 2019;7:183.
- Chan TA, Yarchoan M, Jaffee E, Swanton C, Quezada SA, Stenzinger A, Peters S. Development of tumor mutation burden as an immunotherapy biomarker: utility for the oncology clinic. *Ann Oncol* 2019;30:44-56.
- Chalmers ZR, Connelly CF, Fabrizio D, Gay L, Ali SM, Ennis R, et al. Analysis of 100,000 human cancer genomes reveals the landscape of tumor mutational burden. *Genome Med* 2017;9:34.
- Hellmann MD, Paz-Ares L. Lung Cancer with a High Tumor Mutational Burden. *N Engl J Med* 2018;379:1093-4.
- Li M, Li X, Guo Y, Miao Z, Liu X, Guo S, Zhang H. Development and assessment of an individualized nomogram to predict colorectal cancer liver metastases. *Quant Imaging Med Surg* 2020;10:397-414.
- Attanasio S, Forte SM, Restante G, Gabelloni M, Guglielmi G, Neri E. Artificial intelligence, radiomics and other horizons in body composition assessment. *Quant Imaging Med Surg* 2020;10:1650-60.
- Bodalal Z, Trebeschi S, Nguyen-Kim TDL, Schats W, Beets-Tan R. Radiogenomics: bridging imaging and genomics. *Abdom Radiol (NY)* 2019;44:1960-84.
- Pinker K, Chin J, Melsaether AN, Morris EA, Moy L. Precision Medicine and Radiogenomics in Breast Cancer: New Approaches toward Diagnosis and Treatment. *Radiology* 2018;287:732-47.
- Wang L, Ge J, Lan Y, Shi Y, Luo Y, Tan Y, Liang M, Deng S, Zhang X, Wang W, Tan Y, Xu Y, Luo T. Tumor mutational burden is associated with poor outcomes in diffuse glioma. *BMC Cancer* 2020;20:213.
- Peng X, Yishuang C, Kaizhou Z, Xiao L, Ma C. Conventional Magnetic Resonance Features for Predicting 1p19q Codeletion Status of World Health Organization Grade II and III Diffuse Gliomas. *J Comput Assist Tomogr* 2019;43:269-76.
- Liu Z, Liu H, Liu Z, Zhang J. Oligodendroglial tumours: subventricular zone involvement and seizure history are associated with CIC mutation status. *BMC Neurol* 2019;19:134.
- Park YW, Han K, Ahn SS, Bae S, Choi YS, Chang JH, Kim SH, Kang SG, Lee SK. Prediction of IDH1-Mutation and 1p/19q-Codeletion Status Using Preoperative MR Imaging Phenotypes in Lower Grade Gliomas. *AJNR Am J Neuroradiol* 2018;39:37-42.
- Zhang S, Wu S, Wan Y, Ye Y, Zhang Y, Ma Z, Guo Q, Zhang H, Xu L. Development of MR-based preoperative nomograms predicting DNA copy number subtype in lower grade gliomas with prognostic implication. *Eur Radiol* 2021;31:2094-105.
- Bouffet E, Larouche V, Campbell BB, Merico D, de Borja R, Aronson M, et al. Immune Checkpoint Inhibition for Hypermutant Glioblastoma Multiforme Resulting From

- Germline Biallelic Mismatch Repair Deficiency. *J Clin Oncol* 2016;34:2206-11.
26. Bloch O, Crane CA, Kaur R, Safaee M, Rutkowski MJ, Parsa AT. Gliomas promote immunosuppression through induction of B7-H1 expression in tumor-associated macrophages. *Clin Cancer Res* 2013;19:3165-75.
  27. Preusser M, Berghoff AS, Wick W, Weller M. Clinical Neuropathology mini-review 6-2015: PD-L1: emerging biomarker in glioblastoma? *Clin Neuropathol* 2015;34:313-21.
  28. Liu L, Bai X, Wang J, Tang XR, Wu DH, Du SS, Du XJ, Zhang YW, Zhu HB, Fang Y, Guo ZQ, Zeng Q, Guo XJ, Liu Z, Dong ZY. Combination of TMB and CNA Stratifies Prognostic and Predictive Responses to Immunotherapy Across Metastatic Cancer. *Clin Cancer Res* 2019;25:7413-23.
  29. Schrock AB, Ouyang C, Sandhu J, Sokol E, Jin D, Ross JS, Miller VA, Lim D, Amanam I, Chao J, Catenacci D, Cho M, Braiteh F, Klempner SJ, Ali SM, Fakih M. Tumor mutational burden is predictive of response to immune checkpoint inhibitors in MSI-high metastatic colorectal cancer. *Ann Oncol* 2019;30:1096-103.
  30. McGranahan N, Furness AJ, Rosenthal R, Ramskov S, Lyngaa R, Saini SK, et al. Clonal neoantigens elicit T cell immunoreactivity and sensitivity to immune checkpoint blockade. *Science* 2016;351:1463-9.
  31. Wei J, Yang G, Hao X, Gu D, Tan Y, Wang X, Dong D, Zhang S, Wang L, Zhang H, Tian J. A multi-sequence and habitat-based MRI radiomics signature for preoperative prediction of MGMT promoter methylation in astrocytomas with prognostic implication. *Eur Radiol* 2019;29:877-88.
  32. Broen MPG, Smits M, Wijnenga MMJ, Dubbink HJ, Anten MHME, Schijns OEMG, Beckervordersandforth J, Postma AA, van den Bent MJ. The T2-FLAIR mismatch sign as an imaging marker for non-enhancing IDH-mutant, 1p/19q-intact lower-grade glioma: a validation study. *Neuro Oncol* 2018;20:1393-9.
  33. Wang J, Zheng X, Zhang J, Xue H, Wang L, Jing R, Chen S, Che F, Heng X, Li G, Xue F. An MRI-based radiomics signature as a pretreatment noninvasive predictor of overall survival and chemotherapeutic benefits in lower-grade gliomas. *Eur Radiol* 2021;31:1785-94.
  34. Tay KL, Tsui A, Phal PM, Drummond KJ, Tress BM. MR imaging characteristics of protoplasmic astrocytomas. *Neuroradiology* 2011;53:405-11.
  35. Alghamri MS, Thalla R, Avvari RP, Dabaja A, Taher A, Zhao L, Ulintz PJ, Castro MG, Lowenstein PR. Tumor mutational burden predicts survival in patients with low-grade gliomas expressing mutated IDH1. *Neurooncol Adv* 2020;2:vdaa042.
  36. Samstein RM, Lee CH, Shoushtari AN, Hellmann MD, Shen R, Janjigian YY, et al. Tumor mutational load predicts survival after immunotherapy across multiple cancer types. *Nat Genet* 2019;51:202-6.
  37. Hwang WL, Wolfson RL, Niemierko A, Marcus KJ, DuBois SG, Haas-Kogan D. Clinical Impact of Tumor Mutational Burden in Neuroblastoma. *J Natl Cancer Inst* 2019;111:695-9.
  38. Saini A, Breen I, Pershad Y, Naidu S, Knuttinen MG, Alzubaidi S, Sheth R, Albadawi H, Kuo M, Oklu R. Radiogenomics and Radiomics in Liver Cancers. *Diagnostics (Basel)* 2018;9:4.
  39. Story MD, Durante M. Radiogenomics. *Med Phys* 2018;45:e1111-22.
  40. Zhao J, Ma W, Zhao H. Loss of heterozygosity 1p/19q and survival in glioma: a meta-analysis. *Neuro Oncol* 2014;16:103-12.
  41. Xia L, Wu B, Fu Z, Feng F, Qiao E, Li Q, Sun C, Ge M. Prognostic role of IDH mutations in gliomas: a meta-analysis of 55 observational studies. *Oncotarget* 2015;6:17354-65.
  42. Zanfardino M, Pane K, Mirabelli P, Salvatore M, Franzese M. TCGA-TCIA Impact on Radiogenomics Cancer Research: A Systematic Review. *Int J Mol Sci* 2019;20:6033.

**Cite this article as:** Liu ET, Zhou S, Li Y, Zhang S, Ma Z, Guo J, Guo L, Zhang Y, Guo Q, Xu L. Development and validation of an MRI-based nomogram for the preoperative prediction of tumor mutational burden in lower-grade gliomas. *Quant Imaging Med Surg* 2022;12(3):1684-1697. doi: 10.21037/qims-21-300